*Article*

# How to Improve an Offshore Wind Station

**João Paulo N. Torres** [1,2,*] , **Ana Sofia De Jesus** [3] and **Ricardo A. Marques Lameirinhas** [1,3,*]

1   Instituto de Telecomunicações, 1049-001 Lisbon, Portugal
2   Academia Militar/CINAMIL, Av. Conde Castro Guimarães, 2720-113 Amadora, Portugal
3   Department of Electrical and Computer Engineering, Instituto Superior Técnico, 1049-001 Lisbon, Portugal; ist186940@tecnico.ulisboa.pt
*   Correspondence: joaoptorres@hotmail.com (J.P.N.T.); ricardo.lameirinhas@tecnico.ulisboa.pt (R.A.M.L.)

**Abstract:** The ocean is approximately 71% of the Earth's surface and has a lot of resources available. Nowadays, human beings are looking for renewable ways to obtain energy. Offshore power can be obtained in several different ways. Offshore wind power is the most used renewable offshore energy. Since 2017, offshore wind power has a competitive price in comparison with conventional sources. In the 2010s, offshore wind power grew at over 30% per year. Although it has remained less than one percent of the overall world electricity generation, offshore wind power becomes quite relevant on the northern European countries from 2020. However, there are other ways to obtain energy offshore such as using tides and the sun. These types of farms are expensive and difficult to install and, therefore, we propose a combination of several renewable energies in one farm. The main ambition of this work is to try to reduce the installation and maintenance costs of the two types of offshore renewable energies by creating a structure capable of supporting the two types of turbines. To accomplish it, a theoretical study will be made, a brief state-of-the-art will be presented, the chosen items and the environment chosen for installation will be referred to, a prototype will be simulated using a multiphysics software and, finally, the results and conclusions will be presented, based on a Portuguese case study. How piezoelectric materials can enter offshore farms to increase efficiency is also referred to. The project proved to be possible of producing approximately 12.5 GWh of energy annually, more or less enough to supply 10 thousand homes. However, the installation of the piezoelectric materials did not prove to be viable as it is an expensive technology and does not produce a large amount of energy.

**Keywords:** co-located offshore renewable energies; piezoelectricity; tidal power; wind power

## 1. Introduction

All over the world, nations are facing challenges in finding the best way to obtain energy. There are a global need for energy and mineral resources, which has been increasing year after year caused by the technological advances. The study reveals that the natural reserve of fossil fuels represents 150 years (coal), 58 years (natural gas) and almost 46 years (oil) of consumption at current rates. Fossil fuels are by definition a finite source (or at least, Humans consume that energy faster the it is renewed). Meanwhile, the pollution they cause (from climate-damaging greenhouse gases to health-endangering particles) has been setting negatively records, leading to dramatic consequences [1–3].

The world has an abundant source of natural, clean power derived from the wind, waves, tides, sun and others. Ocean, which covers approximately 71% of the Earth's surface, is seen as a huge opportunity. Offshore renewable are worldly recognised as reliable and stable electricity sources. Also, they are seen as support for water desalination and aquaculture [1–4].

The development of renewable technologies, associated to the global energy transition, promises to spur new industries, leading to jobs creation. Wind is the most explored and investigated offshore source. In 1991 was installed in Denmark the world's first offshore

wind farm. Nowadays, millions of people consumes electricity from large-scale offshore wind farm projects [1–4].

The growth of European offshore wind, since the early 2000s, is supported by a steadily fallen over the years. In 2016, 10 European countries had already more than 12 MW grid-connected production from 81 offshore wind farms, with a total of 3589 turbines installed. Nowadays, based on several signed commitments to reduce greenhouse gases emissions as well as the targets to reach carbon neutrality led to promising prediction regarding these renewable technologies [1–4].

It is estimated that the objective to have an installed capacity of at least 60 GW of offshore wind and at least 1 GW of ocean energy by 2030, with a view of reaching 300 GW and 40 GW of installed capacity, respectively, by 2050 is realistic and achievable. In addition to offshore wind energy, there are other ways to produce energy offshore [2,3].

Market forces, technological advances and price developments will continue to drive offshore renewable energy growth over the coming years. However, there are some obstacles. Offshore farms can be expensive and difficult to build and maintain. Therefore, we have to take advantage and get the best out of this installation. Wind, sun and tides are unlimited resources that we can gather offshore. Therefore, the analysis and study of possible farms that can generate all of these types of energy together is an interesting and attractive research theme [2,3].

## 2. Overview and State-of-the-Art

Wind power or wind energy is an energy type that uses the kinetic energy of the wind and converts it to mechanical energy through wind turbines to turn electric generators for electrical power. The power content of the column of air is expressed by [2,3]:

$$P_{wind} = \frac{1}{2}\rho A v^3 \tag{1}$$

where $\rho$ is the fluid density, $A$ the cross-sectional area and $v$ the fluid velocity. Figure 1 illustrates this.

Betz's law indicates the maximum power that can be extracted from the wind, independent of the design of a wind turbine in open flow.
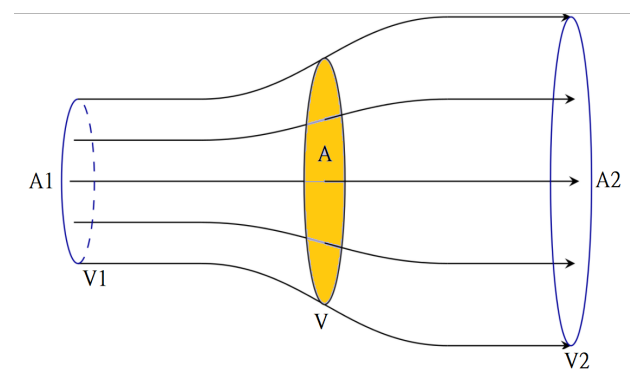


**Figure 1.** Schematic of fluid flow through a disk-shaped actuator. For a constant density fluid, the cross-sectional area varies inversely with speed.

The actual mechanical power $P$ extracted by the rotor blades in watts is the difference between the upstream and the downstream wind powers:

$$P = \frac{1}{2}\rho A v(v_1^2 - v_2^2) \tag{2}$$

where $v = \frac{v_1 + v_2}{2}$. We can calculate the power obtainable from a cylinder of fluid with cross-sectional area $S$ and velocity $v_1$:

$$P = C_p \frac{1}{2} \rho A v_1^3 \tag{3}$$

where $C_p$ is the power coefficient.

An offshore and an onshore wind turbine have similar technology. They diverge on the fact that offshore ones might produce more energy: higher wind speeds are available offshore comparing to on land, so offshore wind power's electricity generation is higher per amount of capacity installed.

Portugal only has 2 MW of offshore capacity in the floating wind turbine WindFloat near the Aguçadoura Wave Farm in Povoa de Varzim.

Tidal energy is power produced by the surge of ocean waters during the rise and fall of tides, where the intensity of the water from the rise and fall of tides is a form of kinetic energy.

Tidal stream generators draw energy from water currents in the same way wind turbines draw energy from air currents. The water density is about 800 times the density of air. This means that a single generator can provide significant power at low tidal flow velocities compared with similar wind speeds [5].

Piezoelectricity is the process of using crystals to convert mechanical energy into electrical energy, or vice versa, so there are two types of piezoelectric effect, direct piezoelectric effect and inverse piezoelectric effect. Since wind pressure is exerted on the wind turbine blades, the blades can be filled with piezoelectric materials to maximize the power obtained by wind force. When the wind impacts the piezoelectric panel, the change of pressure caused by the wind power is output as the voltage through the measuring meter and converted into the amount of energy [6].

The main objective of the co-location of offshore wind and tidal stream turbines is to reduce the cost of electricity generation from either technology separately [7–9].

Thus far, there is no yield that combines these two types of energy. However, there are some studies that simulate this installation.

A case-study site in the Pentland Firth that uses an eddy viscosity wake model in OpenWind to assess Wind energy, with a 3 MW rated power curve and thrust coefficient from a Vestas V90 turbine and to assess tidal energy, "is modeled using a semi-empirical superposition of self-similar plane wakes with a generic 1 MW rated power curve and thrust based on a full-scale, fixed-pitch turbine" [10].

The support structure loads due to wind, waves and current on a combined support structure featuring a single 3 MW wind turbine and 1 MW tidal turbine have been modeled for the same co-located farm case study of the Inner Sound of the Pentland Firth.

In this study, it has shown that the potential to share support structures by adding a tidal turbine to a wind turbine support looks promising.

This co-location results in a 70% increase in energy yield compared to operating the tidal turbines alone. It is found that, "within the space required around a single 3 MW wind turbine, co-location provides a 10–16% cost saving compared to operating the same size tidal-only array without a wind turbine. Furthermore, for the same cost of electricity, a co-located farm could generate 20% more yield than a tidal-only array" [7]. This also could help tidal stream technology move from being commercially uncompetitive alone to competitive when co-located with the wind [7,10].

There is other research that focuses on proposing and evaluating an optimized hybrid wind system and tidal turbines operating as a renewable energy generating unit in New Zealand.

It is known that using the capacities of wind and tidal power in renewable technologies would be a suitable alternative for fossil fuels and would help to prevent their detrimental effects on the environment. It is a cost-effective procedure for the power generation sector to maximize these renewables as a hybrid system.

This research indicates that Kaipara harbor has good potential for energy generation from a hybrid system (wind plus tidal) with good wind energy yield and additional energy from tidal energy.

It is concluded that the installation of a hybrid system with wind and tidal energy in a certain place in New Zealand is beneficial. However, prototypes would have to be installed to complete this study [11].

Another study, which uses the coast of the United Kingdom, is considered. This co-location of wind and tidal power will offer synergies of shared infrastructures that will help to reduce both capital and operational costs. With this purpose, a simulation and modeling of the system in terms of generation, structural forces, integration to the grid and economics is performed.

Although having Levelized Cost of Energy (LCOE) higher than a normal offshore wind farm, the co-location of both technologies are demonstrating feasible. The advantages of the use of tidal are that we can produce a lot of reliable energy with smaller turbines and seize more energy from the same location [1,12].

This study proposes a single structured tower with hybrid renewable energy cultivation on the southwest coast of Yemen.

### 3. Environment Chosen for Installation

The proposed installation will be simulated in the atmospheric conditions of Povoa de Varzim in Viana do Castelo, where the WindFloat Atlantic project is installed. The average wind speed in this location is presented in Figure 2.
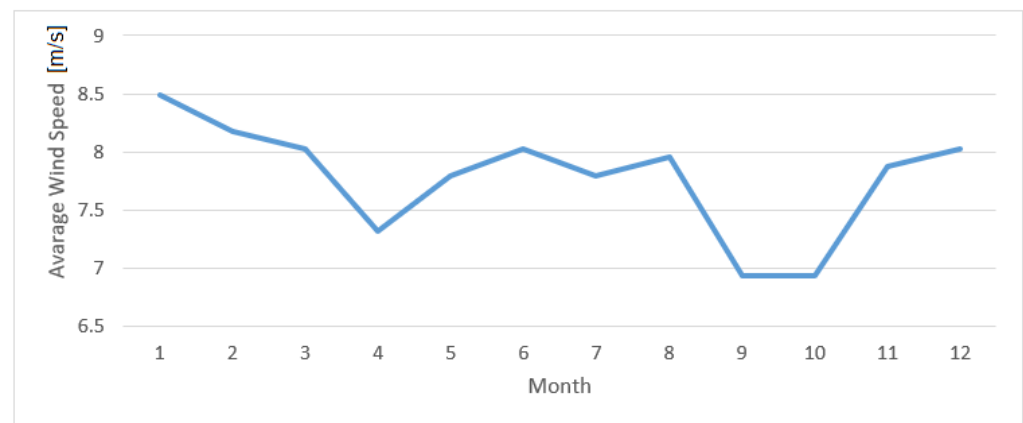


**Figure 2.** Wind Speed (m/s) Variability at 100 m high.

In the following figure, we can see how the average wind speed varies during a year at the height of 100 m. This information was provided by the Global Wind Atlas website.

The data collected is for a height of 100 m, and our rotor is about 190 m high. The following equation, the logarithmic profile law, can determine the wind speed at a certain height, which is used to compute the values on Table 1.

$$v_h = v_{an} \times \left| \frac{ln(Z_h/z_0)}{ln(Z_{an}/z_0)} \right| \tag{4}$$

where $v_h$ is the e velocity at the desired height $Z_h$, $v_{an}$ is the velocity at the anemometer height $Z_{an}$ and $z_0$ is the surface roughness length, which is 0.005 m/s for the blown sea [13].

Unlike what happens with the wind, obtaining information about the currents' speed is very difficult. This information is scarce and hard to find. This information was provided by the Instituto Hidrografico (IH), which provided data on current speeds in 2015 at the chosen location.

**Table 1.** Wind Speed at 100 m and 190 m.

|  | Wind Speed at 100 m | Wind Speed at 190 m |
|---|---|---|
| Minimum | 5.61 m/s | 5.97 m/s |
| Average | 7.78 m/s | 8.28 m/s |
| Maximum | 10.52 m/s | 11.20 m/s |

Only the maximum and average values, on Table 2 of the current speed will be considered as the minimum value is null.

**Table 2.** Current speed.

|  | Current Speed at 40 m Deep |
|---|---|
| Average | 1.512 m/s |
| Maximum | 1.920 m/s |

## 4. Modelation

The wind turbines used in the simulation will be identical to those used in the Wind-Float Atlantic project located in Povoa de Varzim because it is the only project of offshore wind energy in Portugal. The WindFloat Atlantic project has three V164-8.4 MW wind turbines mounted on the semi-submersible WindFloat platforms that are anchored to the seabed at a water depth of 100 m.

In the proposed project, we will use a turbine with the same specifications that an AR1500 tidal turbine. After analyzing the characteristics of PVDF and PZT, the piezoelectric materials chosen to apply in the structure were the PVDF. The PVDF model chosen was PROWAVE FS-2513P SENSOR, PIEZO FILM [14].

## 5. Calculations

To know the power generated by the turbines, we need to know the wind and the current speed, the surface area of the blades, the fluid density and the power coefficient, which varies with wind and current speed.

The equation that allows us to obtain the power has already been mentioned previously (3). For our wind speed values, results are presented on Table 3.

**Table 3.** Values of $C_p$ according to chosen wind speeds.

| Wind Speed (m/s) | Power Coefficient |
|---|---|
| 5.97 | 0.41 |
| 8.28 | 0.44 |
| 11.20 | 0.44 |

The blade's surface area is given by $\pi r^2$, 21,124 m$^2$, where the radius of the surface is 82 m. The normally considered value of air density will be used in these calculations; 1.2225 Kg/m$^3$. The power estimated for different wind speeds is presented on Table 4.

**Table 4.** Values of Power according to wind speed.

| Wind Speed (m/s) | Power (MW) |
|---|---|
| 5.97 | 1.129 |
| 8.28 | 3.232 |
| 11.20 | 7.970 |

Calculating the energy produced during a year, a maintenance period of 15 days was considered when the turbines are not working. At rated power (8 MW), the energy produced would be 16,800 MWh a year. At average power (3.232 MW), the energy produced would be 11,946 MWh a year.

To know the power generated by the tidal turbines we use the same equation but with different data.

The power coefficient for the chosen tidal turbine is not known. Through a study of some different tidal turbines, it was estimated that the power coefficient would be approximately 0.4, and that is the value used in the calculations.

Tidal turbines are also significantly smaller than wind turbines, and because of that, the blade's surface area is also smaller, with a radius of 9 m and a surface area of 254,469 m$^2$

For tidal turbines, the fluid considered is water, and the fluid density is 999 kg/m$^3$. The power estimated for different wind speeds is on Table 5.

**Table 5.** Values of power according to current speed.

| Current Speed (m/s) | Power (kW) |
| --- | --- |
| 1.512 | 175.746 |
| 1.902 | 349.834 |

Calculating the energy produced during a year, a maintenance period of 15 days was considered when the turbines are not working. At rated power (1.5 MW), the energy produced would be 5040 MWh a year. At average power (175.746 kW), the energy produced would be 591 MWh a year.

*5.1. Simulations*

To simulate the proposed structure, where tidal and wind turbines will be installed, as well as piezoelectric materials, it is necessary to simulate some conditions such as wind flow and pressure around the structure.

A 3D model of the structure was constructed using Geometry tool provided by the software.

To make the process easier, the structure was built in parts, and then all the parts were joined as presented on Figure 3. The wind blade has been modeled in 3D and is only a geometric approximation of a real blade due to 3D design software limitations. The blade is 82 m long (actual length of the model Vestas V164-8.0). The tidal turbine was designed using the same base as the wind turbine blade. The tidal turbine is significantly shorter, with each blade just 9 m long, but it is wider and stronger. The floating platform used in the WindFloat project was also designed. Each pole is 30 m high, being 50 m apart. The main tower is 190 m high and joins all of the designed components.
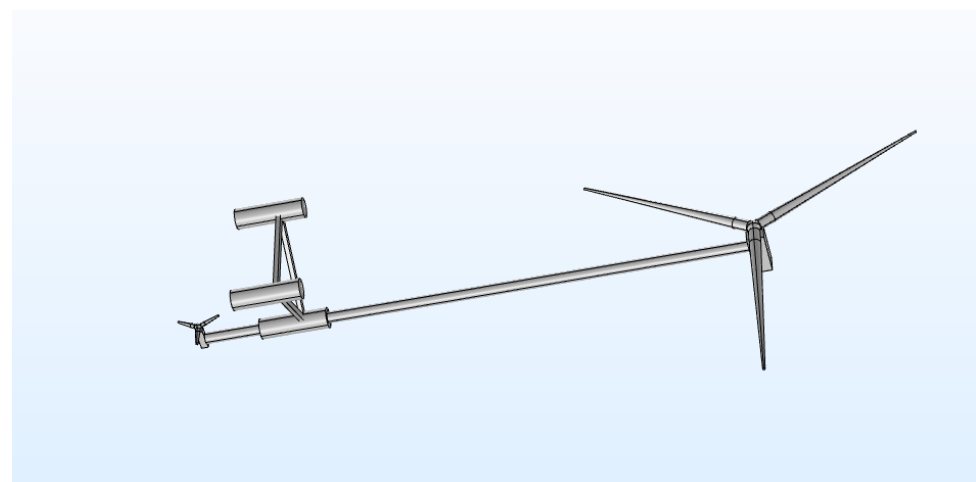


**Figure 3.** Structure drawn using the software.

In order to proceed with the simulations, it is necessary to attribute materials to the designed structures. The structure is made of different materials, including being coated by anti-corrosion materials due to the corrosive effect of water and rain, but it is mainly composed of iron, so the material chosen for all of the structure was iron.

*5.2. Wind Tunnel Simulation*

The wind flow around the structure will be simulated using the software turbulent flow. This module aims to solve the Navier–Stokes equations presented in (5) by modeling the fluid domain around the airflow as a mesh of discrete elements. The set of Equations (5) counts with the fluid density $\rho$, the fluid velocity $\mathbf{u}$, the fluid pressure $p$ and the fluid dynamic viscosity $\mu$. The finer the mesh, the more precise the results are. However, it is always a trade off, as thinner mesh elements imply more computation time. Due to this, the smallest geometry details were removed using the "Cleanup" tool. The equations will be evaluated using a computational assessment technique. Up-to-date, there are three different techniques: Direct Numerical Simulation (DNS), which solves all the eddies, from the largest to the smallest, Large Eddy Simulation (LES), where only the large-scale eddies are resolved and Reynolds-Averaged Navier–Stokes (RANS), a completely different time-averaged method that does not resolve eddies explicitly, choosing to instead model its effect using the concept of turbulent viscosity. RANS is not an explicit method and, therefore, is less computationally expensive, with that being the primary reason for its use in this work [13].

The Navier–Stokes are moment0conservation equations, relating the inertial force $\rho\left(\frac{\partial \mathbf{u}}{\partial t} + \mathbf{u} \cdot \nabla \mathbf{u}\right)$, with the pressure force $-\nabla p$, the viscous forces $\nabla \cdot \left[\mu\left(\nabla \mathbf{u} + (\nabla \mathbf{u})^T - \frac{2}{3}(\nabla \cdot \mathbf{u})\mathbf{I}\right)\right]$ as well as with an external force $\mathbf{F}$.

$$\begin{cases} \rho\left(\frac{\partial \mathbf{u}}{\partial t} + \mathbf{u} \cdot \nabla \mathbf{u}\right) = -\nabla p + \nabla \cdot \left[\mu\left(\nabla \mathbf{u} + (\nabla \mathbf{u})^T - \frac{2}{3}(\nabla \cdot \mathbf{u})\mathbf{I}\right)\right] + \mathbf{F} \\ \frac{\partial \rho}{\partial t} + \nabla \cdot (\rho \mathbf{u}) = 0 \\ \rho = \rho(p, T) \end{cases} \tag{5}$$

After choosing the assessment technique or turbulence model type, a turbulence model needs to be chosen accordingly. For the RANS, the software makes nine different turbulence models available (which can be consulted at the software library). However, for the case study, the *k-ε* turbulence model, where k refers to turbulent kinetic energy and $\epsilon$ the rate of dissipation on turbulent kinetic energy, is selected. Of the reasons behind its election, its good performance for complex geometries, its stability and the possibility to use wall functions stood out. Wall functions are adopted to resolve the thin boundary layer near the wall, preventing the use of a very fine mesh. Essentially, they provide an offset so that the mesh does not need to go near the wall; moreover, being the straightforward solution, a relationship is used to characterize the flow [13].

An incompressible flow approximation is used, assuming the fluid's density as constant, implying that the divergence of the fluid velocity is zero, as suggested in Expression (6). The wind tunnel dimensions are 295 m in height, 200 m in width and 100 m in depth. The above-mentioned structure is placed inside the tunnel. Only the parts of the structure that are inside this wind tunnel are subject to the wind, as illustrated on Figure 4.

$$\nabla \cdot \mathbf{u} = 0 \Rightarrow -\frac{2}{3}(\nabla \cdot \mathbf{u}) = 0. \tag{6}$$

The main goal of the following simulation is to calculate the power generated by the wind turbine by Betz's law and through the equation described above.

As altitude increases, atmospheric pressure decreases. As altitude increases, the amount of gas molecules in the air decreases, and the air becomes less dense than air nearer to sea level. One can calculate the atmospheric pressure at a given altitude. Temperature and humidity also affect the atmospheric pressure. Pressure is proportional to temperature and

inversely proportional to humidity. However, at the height of 190 m, this variation in air pressure is not significant. Therefore, the reference air pressure and temperature were considered, as they are values that do not significantly affect the results. Regarding the wind speed, three different simulations were performed, considering the minimum, average and maximum speed, as in Figure 5. This is the input inserted at the open boundary.
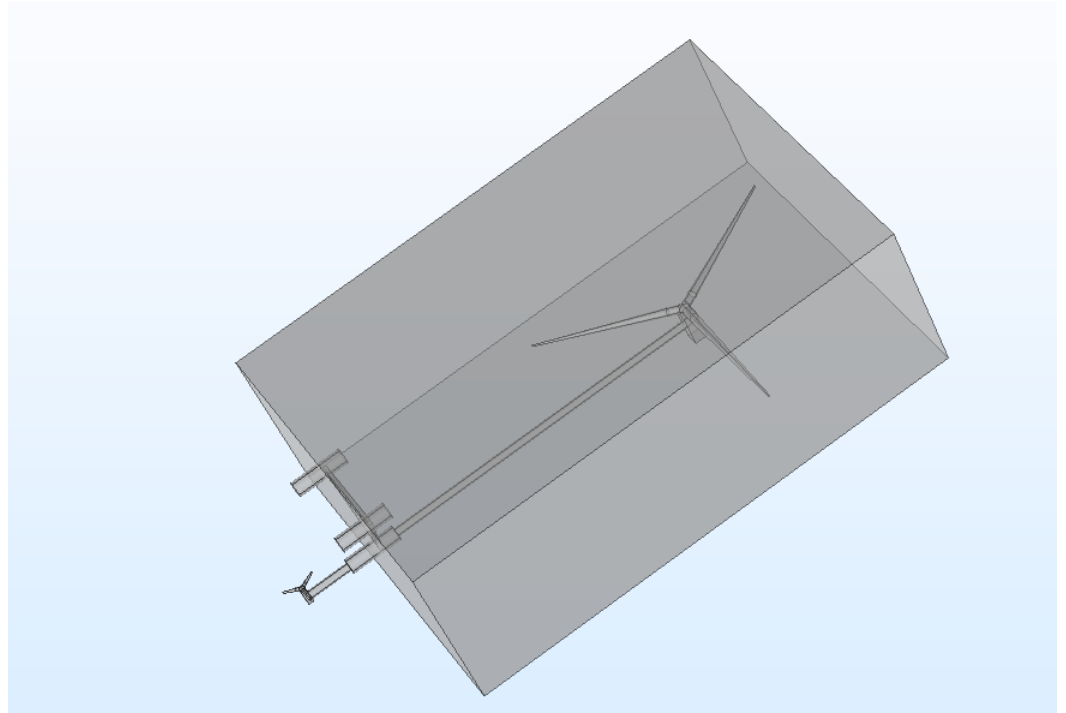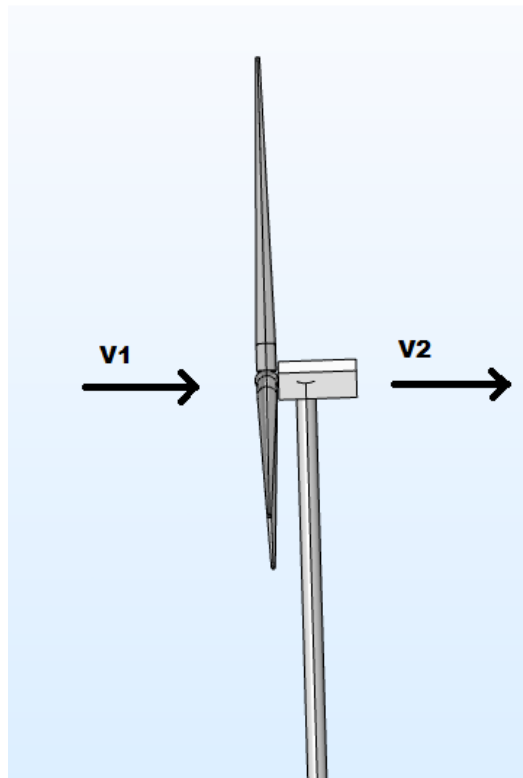


**Figure 4.** Wind tunnel using the software.



**Figure 5.** Betz Law.

In Figure 6, the resulting wind flow is illustrated, being characterized by velocity magnitude, orientation and direction. The velocity magnitude's values are differentiated by colors whose legend can be seen at the right border. This figure is for an input speed of 8.28 m/s, but several simulations were performed for different wind speeds.
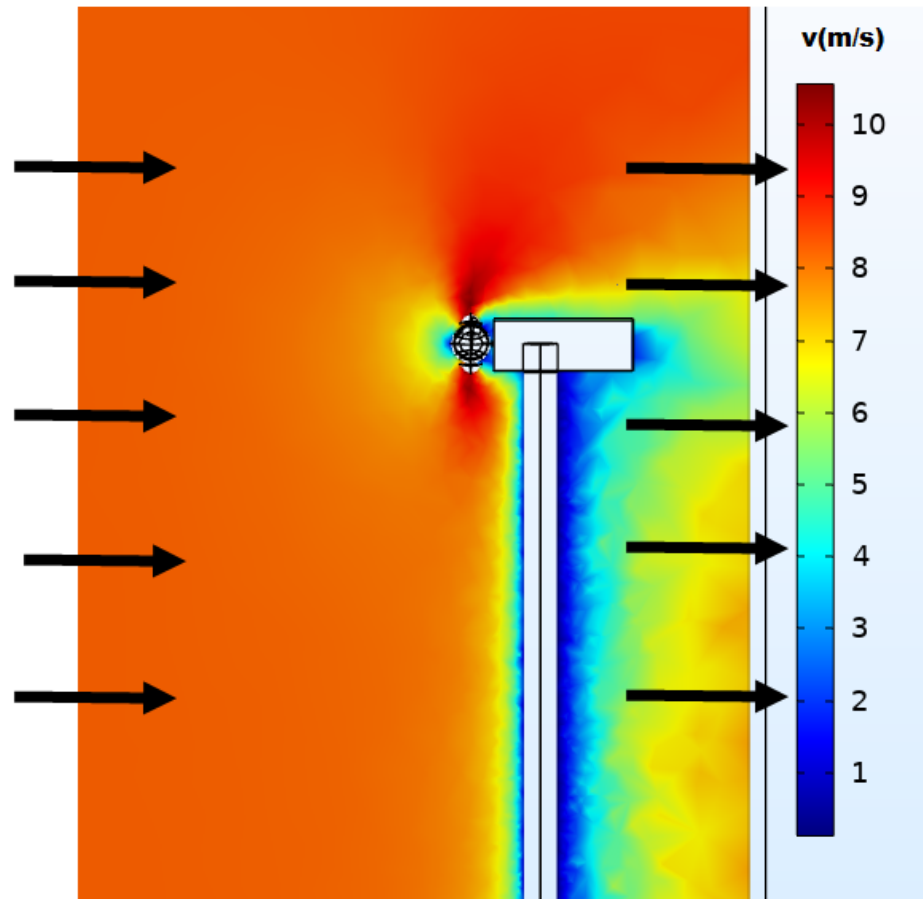


**Figure 6.** Wind speed using the software.

As we have seen before, the main goal is to take $v_2$. The values taken from the performed simulations are shown in Table 6.

**Table 6.** Values of wind speed before and after the rotor.

| Wind Speed $v_1$ (m/s) | Wind Speed $v_2$ (m/s) |
|---|---|
| 5.97 | 4.2 |
| 8.28 | 5.75 |
| 11.20 | 7.78 |

### 5.3. Water Tunnel Simulation

The water flow around the structure will be simulated using the software's turbulent flow. As mentioned before, this module aims to solve the Navier–Stokes equations but instead of air, we are using water.

The water tunnel dimensions are 70 m in height, 200 m in width and 100 m in depth. The above-mentioned structure is placed inside the tunnel. Only the part of the structure that is subject to the water is inside this water tunnel, as presented in Figure 7.
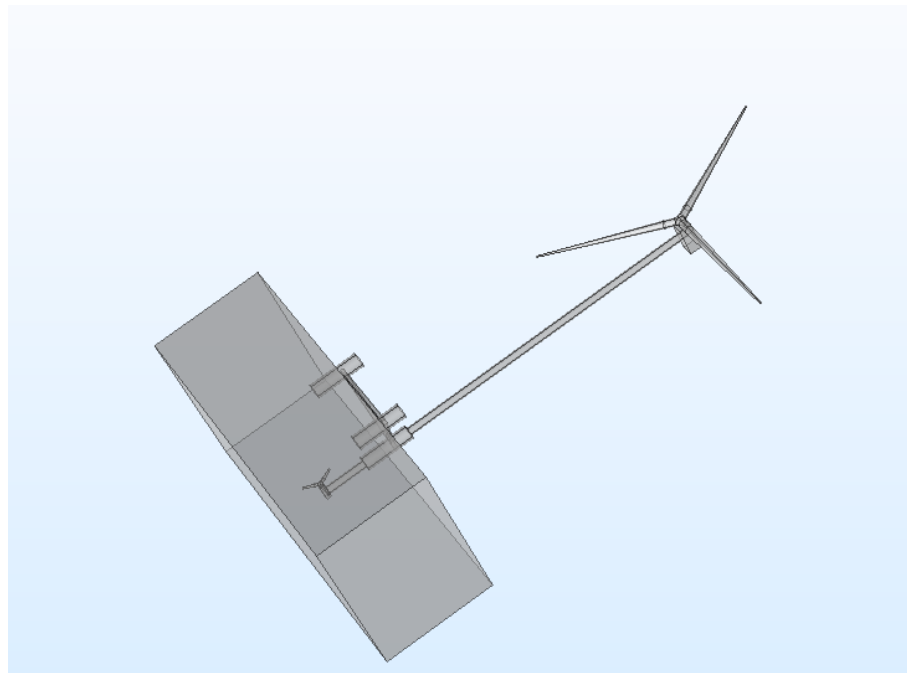
**Figure 7.** Water tunnel using the software.

The concept of the following simulation is the same as the wind turbine simulation. The goal is to obtain $v_2$ to calculate the power generated by the tidal turbine, as presented in Figure 8.
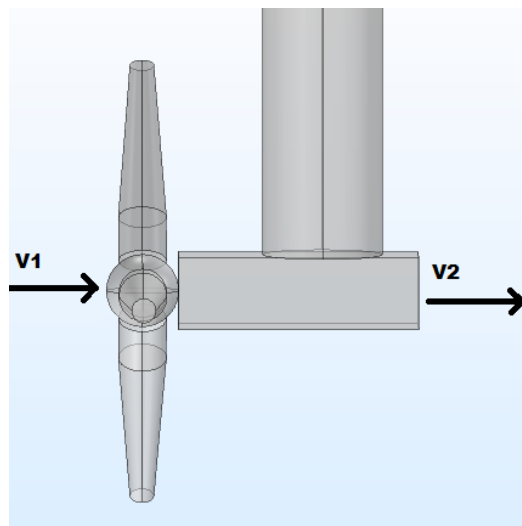


**Figure 8.** Betz Law.

As depth increases, atmospheric pressure also increases. The deeper you go under the sea, the greater the pressure of the water pushing down on you. For every 33 feet (10.06 m) you go down the pressure increases by one atmosphere. The atmospheric pressure at a depth of 40 m is about 5 atm. The water temperature considered will be 10 °C, as it is the average temperature of the water in the chosen place. However, the temperature does not have a considerable effect on the simulation. The average and maximum current speeds were chosen as inputs at the open boundary. Results are on Figure 9.

In the figure above, the resulting water flow is illustrated, being characterized by velocity magnitude, orientation and direction. The velocity magnitude's values are differentiated by colors whose legend can be seen at the right border. This figure is for an input

speed of 1.902 m/s, but several simulations were performed for different current speeds as presented on Table 7.
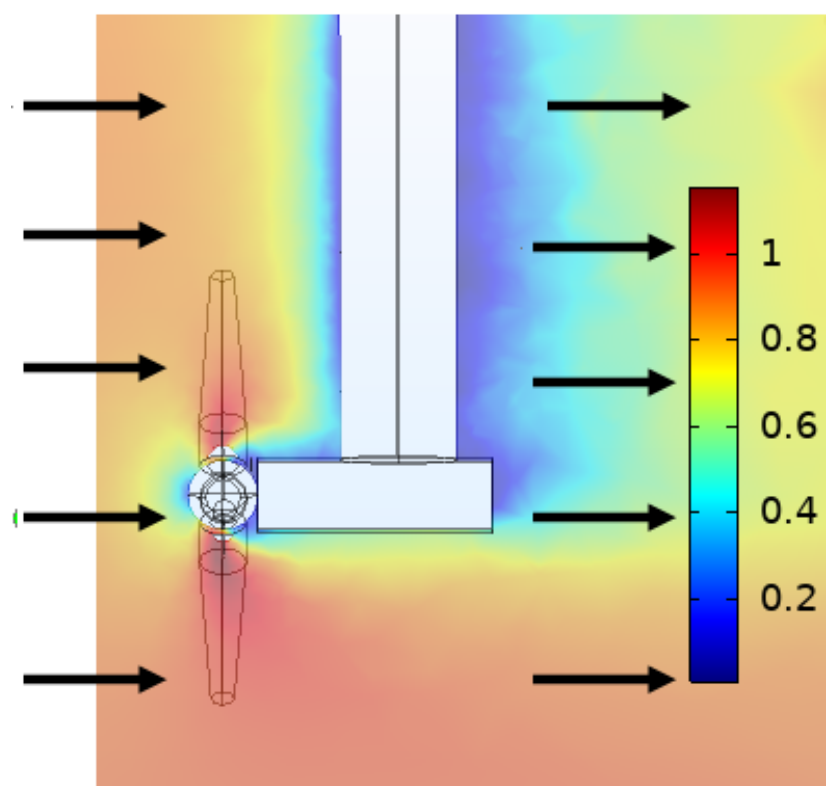


**Figure 9.** Current Speed (m/s) using the software.

**Table 7.** Values of current speed before and after the rotor.

| Current Speed $v_1$ (m/s) | Current Speed $v_2$ (m/s) |
| --- | --- |
| 1.512 | 1.12 |
| 1.902 | 1.35 |

## 6. Piezoelectric Materials Simulation

The piezoelectric effect will be simulated using the software. The piezoelectricity interface combines the solid mechanics and electrostatics interfaces with the constitutive relationships required to model the piezoelectric phenomena. Both direct and inverse piezoelectric effects can be modeled.

The piezoelectric coupling can be formulated using either the strain–charge or stress–charge form. There are three modules within the structural mechanics and acoustics modules branch that offer this feature for simulating piezoelectricity: the acoustics module, MEMS (microelectromechanical systems) and module and structural mechanics module.

The acoustics module includes dedicated tools for modeling wave generation and propagation in fluids, linear elastic materials, porous media and piezoelectric materials. It is used for piezoelectric transducers as transmitters to radiate sound to the surrounding fluids and as receivers to detect sound coming from the surrounding fluids.

The MEMS module includes a terminal feature that allows you to connect a piezoelectric device to an electrical circuit. The electrical circuit can be used to excite the transducer as well as receive detected signals. The terminal feature also enables the computation of the lumped parameters of the piezoelectric device, such as admittance and scattering parameters (S-parameters).

The structural mechanics module provides efficient modeling features such as the shell and membrane interfaces [15].

The simulations will be run by the last module with a geometry as illustrated on Figure 10. This is a finite element analysis (FEA) software package tailored for analyzing the mechanical behavior of solid structures. The structural mechanics module brings built-in multiphysics couplings that include thermal stress, fluid–structure interaction and piezoelectricity [15].

As previously mentioned, the piezoelectric material used is a polyvinylidene difluoride (PVDF) film with an external depth of 13 mm and an external width of 25 mm.
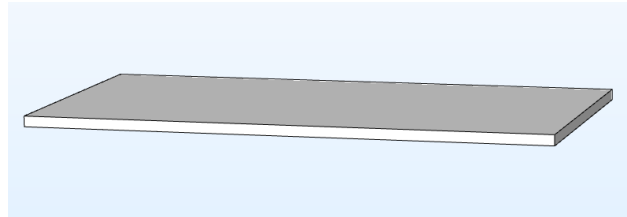


**Figure 10.** PVDF film drawn using the software.

Before any simulation is performed on the piezoelectric material, it is necessary to know the pressure that the wind exerts in the area where the piezoelectric materials will be applied.

The piezoelectric materials will be installed in the area shown in Figure 11.
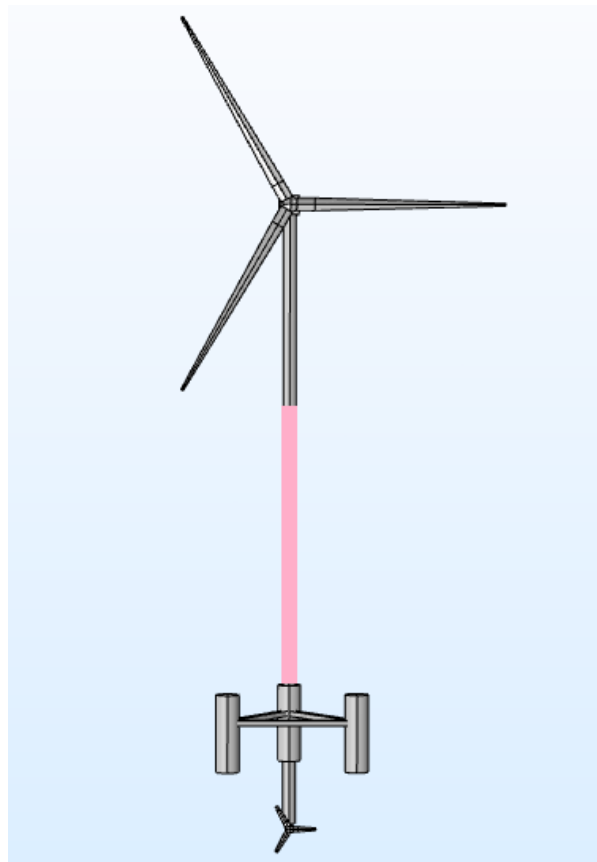


**Figure 11.** Area where piezoelectric materials will be applied.

The piezoelectric materials will be applied in the pink area shown in the figure because they receive the pressure of the wind, and their operation is not significantly affected by the wind turbines. This area is approximately 108 × 2.62 m.

The wind was calculated at the average height of 54 m using the formula mentioned before in Expression (3). Results are compiled on Table 8.

**Table 8.** Values of wind speed at 54 m.

| Wind Speed at 100 m (m/s) | Wind Speed at 54 m (m/s) |
|---|---|
| 5.61 | 5.26 |
| 7.78 | 7.30 |
| 10.52 | 9.87 |

Several simulations were performed to find out the pressure exerted by the wind on the structure. The pressure exerted on the tower with a wind speed of 7.30 m/s is shown on Figure 12 and all the results are compiled in Table 9.
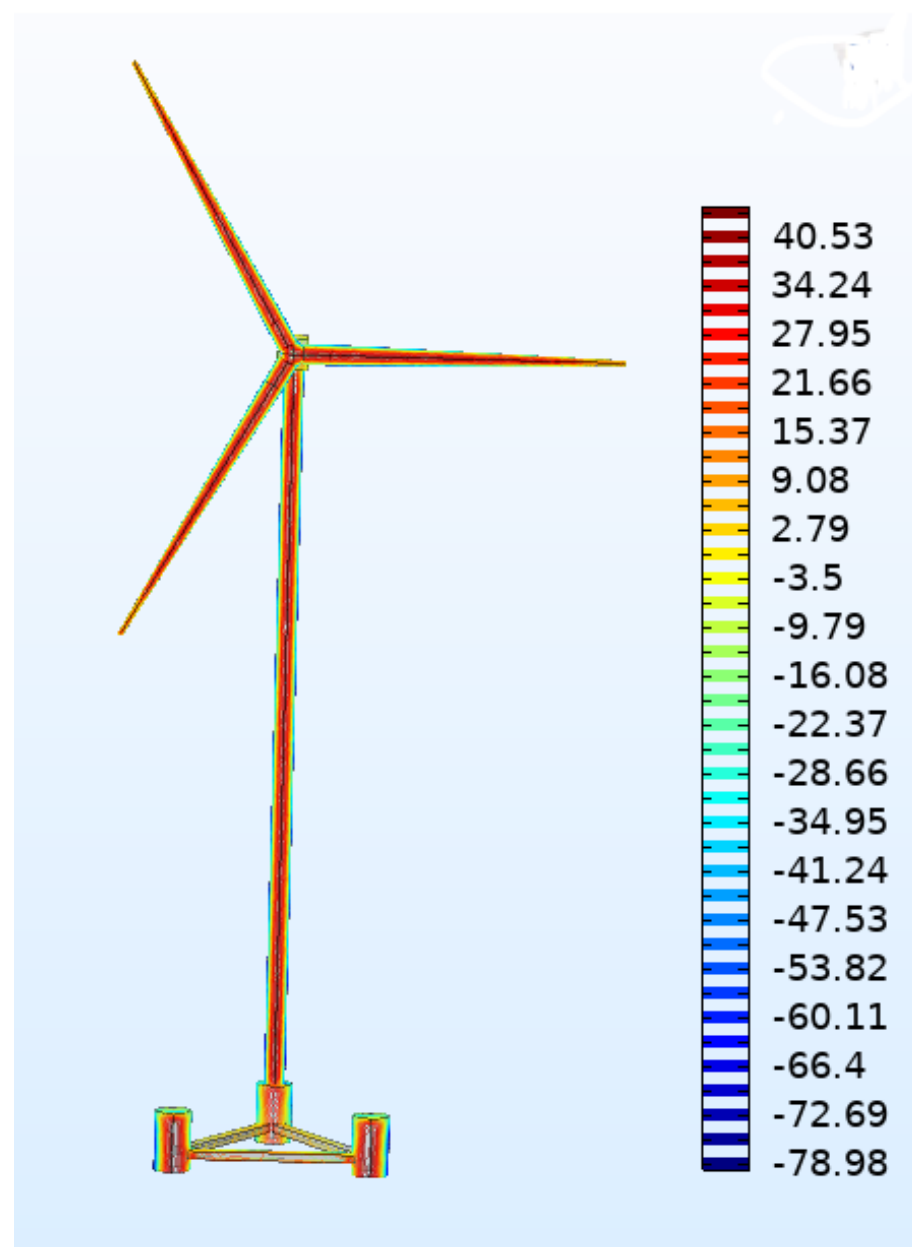


**Figure 12.** Pressure (Pa) using the software.
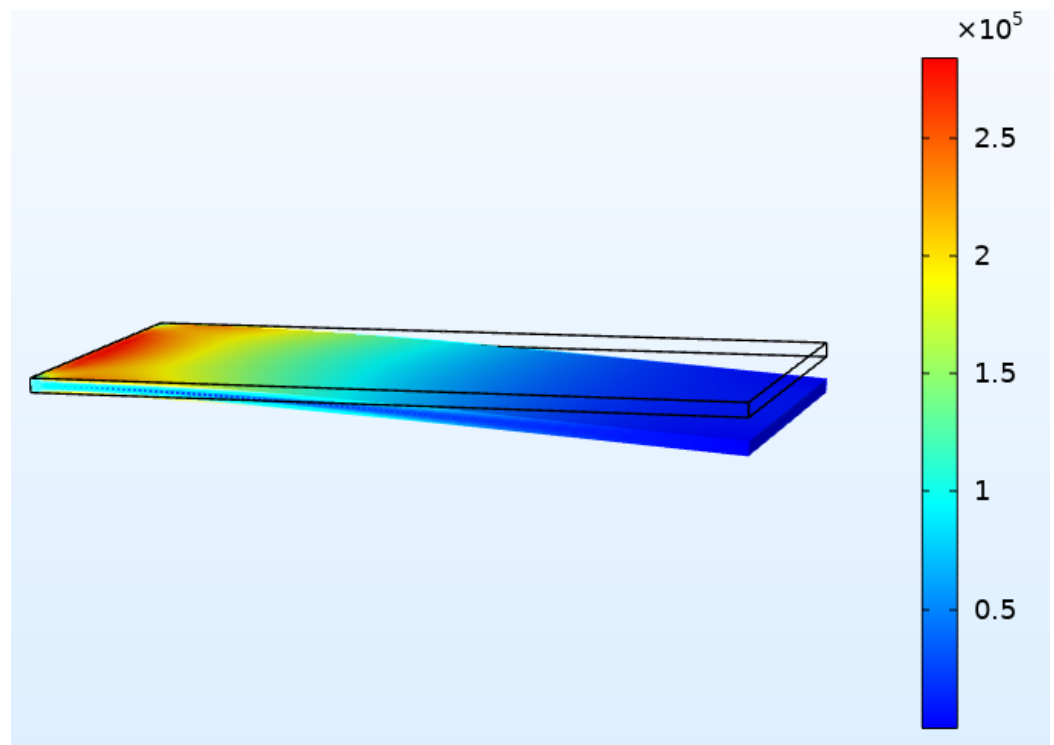
**Table 9.** Values of pressure according to wind speed.

| Wind Speed at 54 m (m/s) | Pressure (Pa) |
| --- | --- |
| 5.26 | 20.010 |
| 7.30 | 38.546 |
| 9.87 | 70.478 |

Knowing the pressure that the wind exerts on the structure, we were able to extract the current density and voltage of the piezoelectric material, presented on Table 10. Therefore, the simulation input is the pressure that we received from the previous simulations.

**Table 10.** Values of voltage and current.

| Pressure (Pa) | Voltage (V) | Current Density Norm (A/m$^2$) |
| --- | --- | --- |
| 20.010 | $1.412 \times 10^{-3}$ | $6.54 \times 10^{-5}$ |
| 38.546 | $1.520 \times 10^{-3}$ | $1.03 \times 10^{-4}$ |
| 70.478 | $2.781 \times 10^{-3}$ | $2.35 \times 10^{-4}$ |

Figure 13 shows the behavior of the piezoelectric material when the wind pressure is exerted.



**Figure 13.** PVDF film stress using the software.

## 7. Results

### 7.1. Wind Turbines

The simulation's main goal is to carry out a comparison between the results calculated theoretically and the results calculated through the simulations performed.

After several simulations were made, where the main goal was to calculate the wind speed at the exit of the rotor, the calculations were carried out to calculate the power generated by the wind turbine.

Through the theoretical equations and with the data taken from the simulations performed, it is possible to calculate the power generated through Equation (2).

To calculate the power generated by the wind turbine, it is necessary to use the following data: $p = 1.225 \text{ kg/m}^3$ and A = 21,124 m$^2$.

Using the data from Table 11, the generated power was calculated. A wind speed of 5.97 m/s corresponds to a power of 1.184 MW, a wind speed of 8.28 m/s corresponds to a power of 3.222 MW, and a wind speed of 11.20 m/s corresponds to a power of 7.970 MW.

**Table 11.** Values of wind speed before and after the rotor.

| Wind Speed $v_1$ (m/s) | Wind Speed $v_2$ (m/s) |
| --- | --- |
| 5.97 | 4.2 |
| 8.28 | 3.232 |
| 11.20 | 7.78 |

To find the power coefficient $C_p$ at a given wind speed, all you have to do is divide the power produced by the total power available in the wind at that speed. Thus, through the simulations and the generated power calculations, we were able to calculate the power coefficient. A wind speed of 5.97 m/s corresponds to a power coefficient of 0.43, a wind speed of 8.28 m/s corresponds to a power coefficient of 0.44, and a wind speed of 11.20 m/s corresponds to a power coefficient of 0.44.

Calculating the energy produced during a year, a maintenance period of 15 days was considered when the turbines are not working. At average power (3.222 MW), the energy produced would be 11909 MWh.

Table 12 shows a comparison between the results obtained theoretically and the results obtained through simulations.

**Table 12.** Comparison of theoretical and simulated results.

| Wind Speed $v_1$ (m/s) | Power Generated (MW) (Theoretical Calculation) | $C_p$ (Theoretical) |
| --- | --- | --- |
| 5.97 | 1.129 | 0.41 |
| 8.28 | 3.232 | 0.44 |
| 11.20 | 7.453 | 0.41 |
| **Wind Speed $v_1$ (m/s)** | **Power Generated (MW) (trough Simulation)** | **$C_p$ (trough Simulation)** |
| 5.97 | 1.184 | 0.42 |
| 8.28 | 3.222 | 0.44 |
| 11.20 | 7.970 | 0.44 |

Analyzing the results obtained, we can see that the theoretical results and those obtained through the simulations are quite similar, which allows us to say that the designed structure has a very close approximation to the real one.

There are several factors that influence the efficiency of a wind turbine. Many aerodynamic factors affect wind turbine power generation, such as wind speed, air density, temperature, air pressure, area swept, and height, etc.

The typical cut-in, rated and cut-out wind-speed values are in the range of 3–5, 10–15 and 25–30 m/s, respectively. The wind turbine chosen has a cut-in wind speed of 4 m/s, a rated wind speed of 13 m/s and a cut-out wind speed of 25 m/s. For the wind speed below the cut-in value, the turbine will produce worthless power. When this happens, the turbines usually enter a parking mode. The turbine is also shut down and kept in parking mode when wind speed is above the cut-out value or during emergency conditions due to

security. For wind-speed values between the cut-in and rated, the power P curve maintains a cubic relationship with respect to wind speed [16]. Figure 14 presents a power curve of a Vestas V164-8.0 turbine.
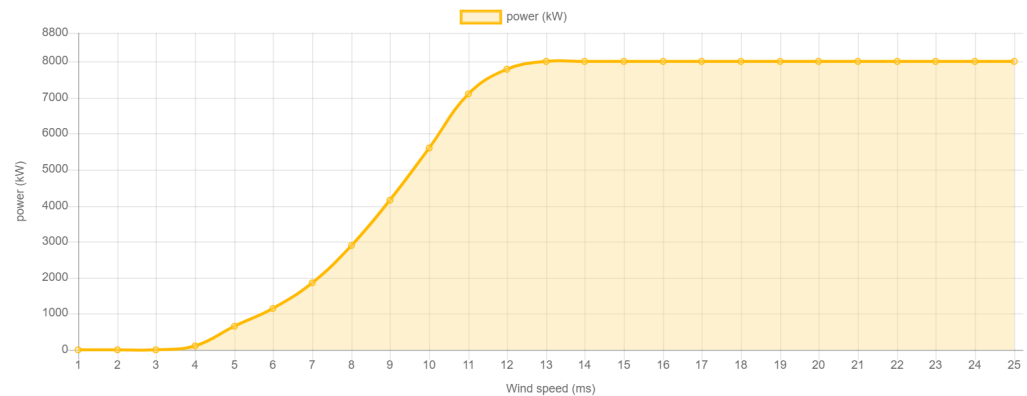


**Figure 14.** Power Curve of Vestas V164-8.0 (from [17]).

Therefore, the location chosen for the installation of these turbines is a good location since the wind speeds practiced in this location are suitable for a good operation of the turbines.

The wind turbine's characteristics are usually related to the degree of air density. The energy produced by the wind is directly commensurate to the degree of air density [16].

Air pressure and temperature affect the air density; they are directly proportional to the pressure and inversely proportional to the temperature. The scale of the pressure and temperature decreases with increasing elevation [16]. However, we saw that the air density does not have a significant change due to temperature and pressure and, therefore, in the simulations, the value of air density was always the same, 1.225 kg/m$^3$.

It is also concluded that the produced power is directly proportional to the rotor-swept area. When the swept area and the diameter of the rotor are large, an increase in energy produced will be earned from the wind.

The tower height is another important factor in the power generated by the turbine. The energy available in the wind is proportional to the cube of the wind speed so any small increase in wind speed will result in an impact on the economic factor. An efficient method to get the turbine in stronger winds is to mount them on taller towers [16].

Near the Earth's surface, friction reduces the wind speed. Frictionless surfaces, such as a quiet sea, offer small amounts of resistance, so the difference in the wind speed with the height is not high. On the other hand, wind undergoes a major change by irregular surfaces, such as forests and buildings [16]. Obstacles such as structures and trees can significantly affect wind speed. They often create turbulence in their neighborhood. The slowdown effect on the wind from an obstacle increases with the height and length of the obstacle. This effect is more pronounced close to the obstacle and close to the ground. It is a good thing to have few major obstacles close to wind turbines, especially in the case they are upwind in the prevailing wind direction, i.e., "in front of" the turbine [16]. Thus, a similar turbine installed at sea or on land with buildings or trees around it will have different efficiency.

The results obtained for these turbines were as expected. Since these turbines are installed in the chosen location, the calculations and results obtained are only a confirmation of the results of the operation of these turbines.

Data provided to the public by EDP (Energias de Portugal) say that a turbine installed at the chosen location generates around 25 GWh during a year. Through our calculations, this result is a little lower, about 12 GWh a year. This difference is due to the fact that we do not use results from real wind speeds and only approximations. The wind speeds used are annual averages of the wind speeds practiced annually and, therefore, there are wind speeds that we were not able to consider in the calculations performed.

*7.2. Tidal Turbines*

As with the simulations for the wind turbine, the main goal was to calculate the wind speed at the exit of the rotor to calculate the power generated by the currents.

The power equation is the same as for the wind turbine, only changing the data: $p = 999 \text{ kg/m}^3$ and $A = 254.469 \text{ m}^2$.

Using the data from Table 13, the generated power was calculated. A current speed of 0.912 corresponds to a power of 38.492 kW, and a current speed of 1.902 m/s corresponds to a power of 371.006 kW.

**Table 13.** Values of current speed before and after the rotor.

| Wind Speed $v_1$ (m/s) | Wind Speed $v_2$ (m/s) |
| --- | --- |
| 1.512 | 1.12 |
| 1.902 | 1.35 |

To find the power coefficient $C_p$ at a given current speed, all you have to do is divide the power produced by the total power available in the current at that speed. Thus, through the simulations and the generated power calculations, we were able to calculate the power coefficient. A current speed of 1.512 corresponds to a power coefficient of 0.40 and a current speed of 1.902 m/s corresponds to a power coefficient of 0.42.

Calculating the energy produced during a year, a maintenance period of 15 days was considered when the turbines are not working. At average power (1.512 m/s), the energy produced would be 575.744 MWh.

Table 14 shows a comparison between the results obtained theoretically and the results obtained through simulations.

**Table 14.** Comparison of theoretical and simulated results. * This value of Cp is just an approximation due to lack of data.

| Current Speed $v_1$ (m/s) | Power Generated (kW) (Theoretical Calculation) | $C_p$ * (Theoretical) |
| --- | --- | --- |
| 1.512 | 175.746 | 0.40 |
| 1.902 | 349.834 | 0.40 |
| Current Speed $v_1$ (m/s) | Power Generated (kW) (trough Simulation) | $C_p$ (trough Simulation) |
| 1.512 | 172.583 | 0.39 |
| 1.902 | 371.006 | 0.42 |

Analyzing the results obtained, we can see that the theoretical results and those obtained through the simulations are quite similar, like the wind turbine, which allows us to say that the designed structure has a very close approximation to the real one.

Unlike wind turbines, tidal turbines do not have much information. However, we know that its efficiency is also affected by some factors such as current speed, water density, temperature, water pressure, area swept and height, etc.

The tidal turbine chosen has a cut-in current speed of less than 1 m/s, a rated current speed of 3 m/s and a cut-out current speed of 5 m/s. Like the wind turbine, in a current speed below the cut-in value, the turbine will produce negligible power and is usually shut down and entered into parking mode. The turbine will also shut down and be kept in parking mode when current speed is above the cut-out value or during emergency conditions due to security. For current speed values between the cut-in and rated, the power P curve maintains a cubic relationship with respect to the current speed. In Figure 15 is a power curve of a AR1500 tidal turbine.
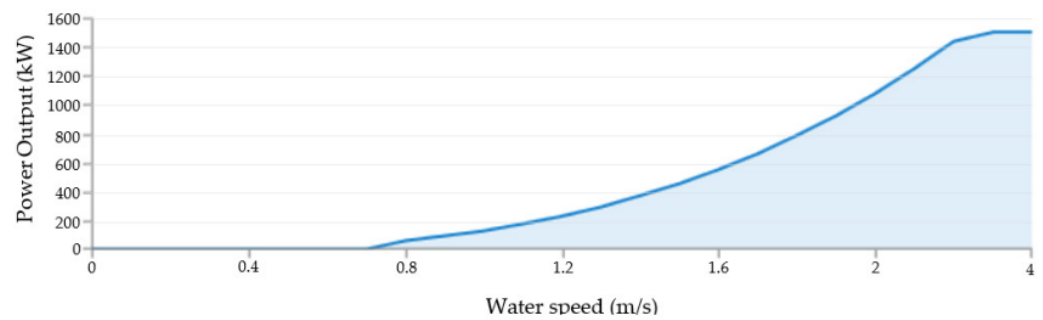
**Figure 15.** Power Curve of AR1500 (from [18]).

The location chosen for the installation of these turbines is not the best since the current speeds practiced in this location are usually lower than the rated current speed. These turbines are normally placed in places where the currents are stronger. However, the current speed in this location is enough for the turbines to properly work.

The energy produced by the current is directly commensurate to the degree of water density. The water density considered was 999 kg/m$^3$. The density does increase with depth, but only to a tiny extent. At the bottom of the deepest ocean, the density is only increased by about 5%, so the change can be ignored in most situations.

It is also concluded that the produced power is directly proportional to the rotor-swept area, just like the wind turbine. When the swept area and the diameter of the rotor are large, an increase in energy produced will be earned from the current.

The current speed changes with depth. Up to a 50 m depth, the current is influenced by the wind. The current speed is normally greatest near the surface.

The tidal turbine's operation is also influenced by the presence of obstacles, and the current speed will be less in the presence of them. However, at sea, the presence of obstacles that influence the operation of the turbines is less likely.

Unlike wind turbines, there is no data on the operation of these tidal turbines in the chosen location. Thus, the results obtained cannot be compared; they can only be analyzed.

*7.3. Piezoelectric Materials*

The purpose of the use of piezoelectric materials is different from the use of wind and tidal turbines. These objects produce a small amount of energy compared to the turbines. They are used to take advantage of the space that exists on the tower and to make the best use of the wind.

Knowing that the available area is approximately 108 × 2.62 m for the application of piezoelectric materials and considering that each piezoelectric has a height of 0.2 mm and a width of 13 mm, we can install a total of 540,200 materials in rows of 200 materials. The materials in each row are connected together in series, and the rows are connected in parallel. This allows that if a material goes bad, only the queue with the material that stops working is affected, making it affect the system as little as possible.

The power generated by piezoelectric materials is only an approximation since these materials produce energy due to pressure fluctuations exerted on them, and these fluctuations are not possible to simulate with the software used. Since this simulation is not possible, this calculation was performed using an approximation. The pressure exerted on the material during 1 s was calculated, and it was assumed that this pressure was the same exerted during the 24 h of a day.

The power calculation is performed through the results taken from the simulation (voltage and current density) and multiplied by the area where the wind pressure is exerted.

After performing these calculations, it is estimated that a generated power of 20 W and daily energy of 480 Wh and 168 kWh a year.

It was seen that the reduced generated power was capable of feeding a lighting signal for a turbine, but the flags found have powers between 30 W and 60 W.

The calculation of the power generated is a calculation based only on the average wind speed occurring at the chosen location and, therefore, it is possible to generate higher power and, in turn, feed an LED light (30 W).

## 8. Conclusions

The main goal of this research work is to understand if there are ways to produce more energy in an offshore wind power station. For this, we studied the possibility of co-localized wind and tidal energy. The possibility of placing piezoelectric materials in the structure was also studied. The costs of this type of technology are quite high and, therefore, the possibility of joining several technologies is a way to reduce the costs of installing these technologies separately and, consequently, we produce more energy. To achieve that, an intensive study of all technologies was made.

First, a viable location was chosen for the installation of the project. There is an offshore wind station on Póvoa de Varzim, and because of that, the location chosen was there. Then, the atmospheric conditions were studied. Subsequently, the necessary items for the proposed infrastructure were chosen. The proposed structure was designed in the software used. The structure designed and simulated to study the co-location of the two types of energy was composed of two types of turbines: AR 1500 Tidal turbine and Vestas V164-8.0 Wind Turbine. Finally, the results obtained after some simulations using the software were discussed.

Through the simulations, we managed to produce a high amount of energy through the installed turbines. As it was calculated, the wind turbine produces a greater amount of energy than the tidal turbine. This is due to the fact that the size of the wind turbine is relatively larger because, for the same turbine dimensions, the tidal turbine can produce a significantly greater amount of energy.

The project proved that it is possible to produce approximately 12.5 GWh of energy annually, more or less enough to supply 10 thousand homes. However, the installation of piezoelectric materials did not prove to be viable as it is an expensive technology and does not produce a large amount of energy. Furthermore, these materials would be exposed to critical atmospheric conditions, which would lead to regular maintenance that is not justifiable.

Green energies are quite expensive energies, and offshore energy is no exception. The biggest disadvantage of this project is undoubtedly the high costs of all components as well as installation and maintenance. The fact that we only performed the simulation for a wind turbine and a tidal turbine helps to increase the project costs. An offshore wind farm pays off if the number of installed turbines is higher because it greatly increases the energy produced, and costs do not increase as much with the increase in turbines.

In conclusion, the project presented is very expensive but a very promising project due to the fact that the technologies used are innovative and produce a large amount of clean energy.

In this study, it was assumed that the platform of the WindFloat project also supports a tidal turbine. The tidal turbine used is a turbine that is supposed to be on the bottom, supported by a structure of its own. A study on whether it would be possible to adapt this turbine to the proposed project and whether the floating platform would be able to support the weight of this turbine will have to be carried out.

A major problem with these facilities is the environmental impact. A study on the impact that the project would have at an environmental level also needs to be carried out.

As for piezoelectric materials, a study on these is also effective. This technology will be a good solution if a piezoelectric material is found that is capable of withstanding difficult atmospheric conditions and capable of being more efficient than the materials proposed in this project.

Lastly and most importantly, a detailed economic analysis would have to be carried out. Most of these projects are quite expensive and do not have detailed budgets available, which leads to great difficulty in projecting a correct budget.

## References

1. Marques Lameirinhas, R.A.; Torres, J.P.N.; de Melo Cunha, J.P. A Photovoltaic Technology Review: History, Fundamentals and Applications. *Energies* **2022**, *15*, 1823. [CrossRef]
2. Ragheb, M.; Ragheb, A.M. Wind Turbines Theory—The Betz Equation and Optimal Rotor Tip Speed Ratio. In *Fundamental and Advanced Topics in Wind Power*; Carriveau, R., Ed.; IntechOpen: Rijeka, Croatia, 2011; Chapter 2. [CrossRef]
3. Ragheb, M.; Ragheb, A.M. *Wind Energy Convertion Theory, Betz Equation*; Wind Energie: Berlin, Germany, 2017.
4. dos Santos Castilho, C.; Torres, J.P.N.; Ferreira Fernandes, C.A.; Marques Lameirinhas, R.A. Study on the Implementation of a Solar Photovoltaic System with Self-Consumption in an Educational Building. *Energies* **2021**, *14*, 2214. [CrossRef]
5. Nachtane, M.; Tarfaoui, M.; Goda, I.; Rouway, M. A review on the technologies, design considerations and numerical models of tidal current turbines. *Renew. Energy* **2020**, *157*, 1274–1288. [CrossRef]
6. Caliò, R.; Rongala, U.B.; Camboni, D.; Milazzo, M.; Stefanini, C.; De Petris, G.; Oddo, C.M. Piezoelectric Energy Harvesting Solutions. *Sensors* **2014**, *14*, 4755–4790. [CrossRef]
7. Lande-Sudall, D.; Stallard, T.; Stansby, P. Co-located offshore wind and tidal stream turbines: Assessment of energy yield and loading. *Renew. Energy* **2018**, *118*, 627–643. [CrossRef]
8. Alfakih, S.; De, T.; Ali, S.; Aneeq, A.; Hayat, K. *Simulation Model of Single Structured Tower Hybrid Wind and Tidal Energy Cultivation Based on Yemen's South West Coast*; EDP Sciences: Les Ulis, France, 2019; Volume 107. [CrossRef]
9. Lande-Sudall, D.; Stallard, T.; Stansby, P. Co-located deployment of offshore wind turbines with tidal stream turbine arrays for improved cost of electricity generation. *Renew. Sustain. Energy Rev.* **2019**, *104*, 492–503. [CrossRef]
10. Lande-Sudall, D. Co-Located Offshore Wind and Tidal Stream Turbines. Ph.D. Thesis, The University of Manchester (United Kingdom), Manchester, UK, 2017.
11. Majdi Nasab, N.; Kilby, J.; Bakhtiaryfard, L. The Potential for Integration of Wind and Tidal Power in New Zealand. *Sustainability* **2020**, *12*, 1807. [CrossRef]
12. Martínez, I.D. Offshore Wind and Tidal Stream Power Plant. Master's Thesis, Universitat Politècnica de Catalunya, Barcelona, Spain, 2019; p. 79.
13. Engana Carmo, J.; Neto Torres, J.P.; Cruz, G.; Marques Lameirinhas, R.A. Effect of the Inclusion of Photovoltaic Solar Panels in the Autonomy of UAV Time of Flight. *Energies* **2021**, *14*, 876. [CrossRef]
14. Riley, M.; Taheri, F.; Islam, M. A critical review of materials available for health monitoring and control of offshore structures. In Proceedings of the 51 st Canadian Chemical Engineering Conference, Halifax, NS, Canada, 14–17 October 2001; pp. 14–17.
15. Piezoelectric Simulations. Available online: https://cdn.comsol.com/wordpress/2014/12/Piezo_COMSOL_50.compressed.pdf (accessed on 20 May 2022).
16. El-Ahmar, M.; El-Sayed, A.H.M.; Hemeida, A. Evaluation of factors affecting wind turbine output power. In Proceedings of the 2017 Nineteenth International Middle East Power Systems Conference (MEPCON), Cairo, Egypt, 19–21 December 2017; IEEE: Piscataway, NJ, USA, 2017; pp. 1471–1476.
17. Models, W.T. Vestas V164-8.0. Available online: https://en.wind-turbine-models.com/turbines/318-vestas-v164-8.0 (accessed on 18 April 2022).
18. Newbold, C.; Akrami, M.; Dibaj, M. Scenarios, Financial Viability and Pathways of Localized Hybrid Energy Generation Systems around the United Kingdom. *Energies* **2021**, *14*, 5602. [CrossRef]